Asymmetric Catalysis at the Mesoscale: Gold Nanoclusters Embedded in Chiral Self-Assembled Monolayer as Heterogeneous Catalyst for Asymmetric Reactions

Elad Gross,[†,§] Jack H. Liu,[†,§] Selim Alayoglu,[†,§] Matthew A. Marcus,[‡] Sirine C. Fakra,[‡] F. Dean Toste,*[,†] and Gabor A. Somorjai*[,†,§]
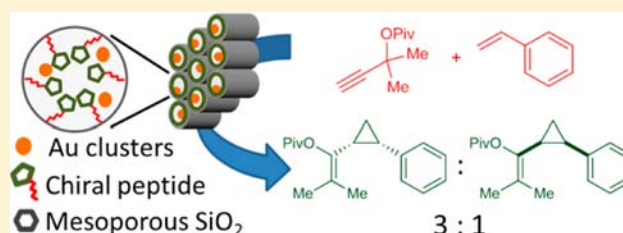
[†]Department of Chemistry, University of California, Berkeley, California 94720, United States

[§]Chemical Sciences Divisions, Lawrence Berkeley National Laboratory, 1 Cyclotron Road, Berkeley, California 94720, United States

[‡]Advanced Light Source, Lawrence Berkeley National Laboratory, 1 Cyclotron Road, Berkeley, California 94720, United States

(S) *Supporting Information*

ABSTRACT: Research to develop highly versatile, chiral, heterogeneous catalysts for asymmetric organic transformations, without quenching the catalytic reactivity, has met with limited success. While chiral supramolecular structures, connected by weak bonds, are highly active for homogeneous asymmetric catalysis, their application in heterogeneous catalysis is rare. In this work, asymmetric catalyst was prepared by encapsulating metallic nanoclusters in chiral self-assembled monolayer (SAM), immobilized on mesoporous SiO_2 support. Using olefin cyclopropanation as an example, it was demonstrated that by controlling the SAM properties, asymmetric reactions can be catalyzed by Au clusters embedded in chiral SAM. Up to 50% enantioselectivity with high diastereoselectivity were obtained while employing Au nanoclusters coated with SAM peptides as heterogeneous catalyst for the formation of cyclopropane-containing products. Spectroscopic measurements correlated the improved enantioselectivity with the formation of a hydrogen-bonding network in the chiral SAM. These results demonstrate the synergetic effect of the catalytically active metallic sites and the surrounding chiral SAM for the formation of a mesoscale enantioselective catalyst.

1. INTRODUCTION

In this work we aimed toward the preparation of catalysts with unique architecture that will utilize the catalytically active metallic site and its surrounding for the formation of highly reactive and selective catalysts. The preparation of these synergetic systems would extend the catalytically active site from the nanoscale to the mesoscale, which implies a principle of operating systems with functions that are beyond the properties of their building blocks.

The development of sophisticated structures for unique catalytic reactivity is widely used in nature. For example, the construction of the three-dimensional structures which can produce high catalytic reactivity and selectivity, including enantioselectivity, is often observed in enzyme-catalyzed reactions.[1]

In homogeneous and heterogeneous catalysis, weak bonds between the reactant and ligands can be essential for highly enantioselective reactions.[2−9] For example, following adsorption of chiral ligands, such as cinchonidine, on the surface of Pt/Al_2O_3, up to 95% enantioselectivity was obtained in hydrogenation of α-ketoester.[3] The catalysts surface was coated by the chiral ligands prior to the reaction, in order to prevent the direct interaction between the metal and the pro-chiral reactant. A specific orientation of the reactant, as it approaches the catalyst, is favored by hydrogen bonding between the cinchonidine ligand and the α-ketoester. These two interactions (reactant−ligand and ligand−metal) were proved to be essential for asymmetric heterogeneous catalytic reactions. As a consequence, the reactants for asymmetric reactions are mainly ketones and aldehydes, in which an oxygen atom, which forms hydrogen bonds with the ligand, is next to the pro-chiral carbon.[3,4] Moreover, the high enantioselectivity was shown to be coupled with a decrease in the reactions rate, due to poisoning of the highly active metallic sites by the strongly adsorbed chiral ligands.[5]

To overcome these limitations, we envisioned the preparation of mesoscale structure in which the enantioselectivity could be achieved by the synthetic analogue of the three-dimensional enzyme's active site. In a similar way to enzymatic systems, the high selectivity would be gained by surrounding the catalytic site with a chiral environment.[8−11] Synthetic chiral supramolecular homogeneous catalysts that are self-assembled through hydrogen bonding show high enantioselectivity for asymmetric organic transformations;[2,8] however, this concept has not been successfully employed for heterogeneous catalysts.

In this paper, we show a new route for the preparation of enantioselective heterogeneous catalyst, in which the metallic

nanoclusters are synthesized within a chiral self-assembled-monolayer (SAM), which is grafted on mesoporous SiO_2 support (MCF-17) without any other stabilizing agent (Au@SAM/MCF-17). By this preparation method, Au clusters are embedded in an interconnected network of chiral molecules, enabling high catalytic reactivity and enantioselectivity for cyclopropanation reactions. It was previously demonstrated that metallic nanoparticles that were embedded or coated by SAM have unique reactivity and selectivity;[12−14] however, chiral SAM was not previously employed for asymmetric catalytic reactions.

In an earlier report, we demonstrated that dendrimer-encapsulated gold nanoclusters are highly active and diastereoselective toward the catalytic formation of cyclopropanes, following the oxidation of nanoclusters by $PhICl_2$ and the formation of highly oxidized Au ions. The diastereoselectivity of the catalytically formed cyclopropane was tuned by the packing density of the dendrimer matrix.[15] Leaching of Au ions to the solution phase was prevented by using toluene as a solvent, due to repulsion between the hydrophobic solvent and the hydrophilic solid catalyst.[15−17] In the current study, the dendrimer matrix was substituted with SAM of chiral molecules immobilized on mesoporous silica support and Au nanoparticles were synthesized within the chiral matrix. Substituting the amino-acid SAM with peptide SAM enhanced the catalytic reactivity, diastereoselectivity, and enantioselectivity. Spectroscopic analysis indicated that highly stabilized SAM was formed by increasing the chain length of the peptides that construct the SAM due to the formation of hydrogen-bonding network in the SAM. These results indicate the importance of the chiral environment that surrounds the metallic site and its role in asymmetric catalytic formation of cyclopropane molecules.

2. RESULTS AND DISCUSSION

2.1. Catalysts Preparation. The synthesis of Au@SAM/MCF-17 is illustrated in Scheme 1. Mesoporous SiO_2 (MCF-

Scheme 1. Preparation of Au Nanoclusters Encapsulated in Chiral SAM/Mesoporous MCF-17 Support
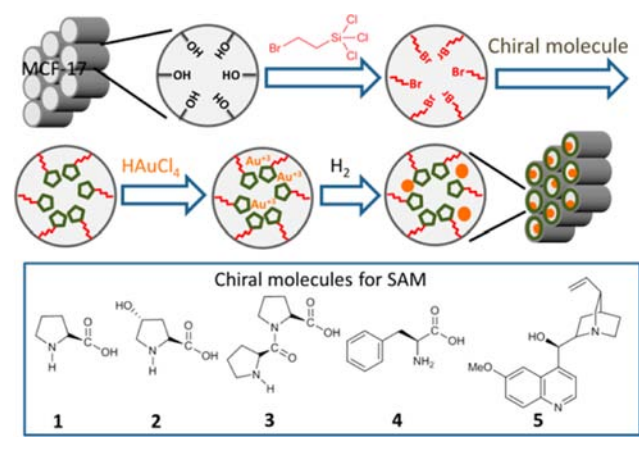
17)[18] was dried under vacuum at 120 °C for 48 h. Bromide-terminated SAM (Br/MCF-17) was prepared by refluxing the dry mesoporous SiO_2 support with $Br(CH_2)_3SiCl_3$ in toluene for 48 h. N_2 BET measurements indicated that following the addition of SAM, the surface area and pore diameter decreased from 525 to 490 $m^2\ g^{-1}$ and 28 to 23 nm, respectively (Supporting Information, Figure S1), with SAM density of 1.8
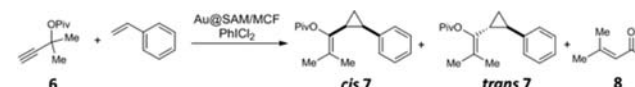
molecule/nm^2.[19] The high density of SAM proved to be essential for the formation of highly selective catalyst. A Br 3d X-ray Photoelectron Spectroscopy (XPS) peak was detected following the formation of Br-terminated SAM (Supporting Information, Figure S2). The high density of the SAM led to a decrease of the SiO-H (850 cm^{-1}) and free O–H (3700 cm^{-1}) signals in Diffusion Reflective Infrared Fourier Transform (DRIFT) spectra (Supporting Information, Figure S3).

Chiral SAM was prepared by alkylation of either (L)-proline **1**, (L)-4 hydroxyproline **2**, (L)-diproline **3**, (L)-phenylalanine **4**, and quinine **5** on Br-terminated SAM/MCF-17 (Scheme 1). For example, Boc-protected (L)-proline **1** was added to Br/MCF-17 with the addition of $K_2CO_3\cdot1.5H_2O$ in THF (followed by the removal of the Boc protecting group). After this step, the surface area and pore diameter of SAM/MCF-17 decreased to 475 $m^2\ g^{-1}$ and 18 nm, respectively (Supporting Information, Figure S1). The quenching of Br 3d signal following the alkylation process indicated that all the surface bromide reacted with the chiral molecules, up to the XPS detection limits (Supporting Information, Figure S2). Characteristic IR peaks of the immobilized chiral molecules were detected in DRIFT spectra (Supporting Information, Figure S3).

Solid-state CP-MAS NMR spectra of Br/MCF-17 indicated the formation of SAM with a terminal halide on the mesoporous silica support (Supporting Information, Figure S4). Following the alkylation of the surface by (L)-diproline (**3**), characteristic carboxylate ester peaks were detected (173 and 65 ppm) along with a decay of the peak correlated to the bromide bearing carbon (34 ppm). Both DRIFTS and CP-MAS NMR spectra verified that the attachment of chiral molecules to the surface was through the carboxylic terminal group.

SAM-directed growth of Au nanoclusters in SAM/MCF-17 was performed (Scheme 1). The Au clusters were synthesized without any stabilizing agent, ensuring that a high percentage of surface atoms would be catalytically accessible. While $HAuCl_4$ was mixed with the chiral SAM/MCF-17 in H_2O, electronic interactions were formed between Au ions and the electron-rich amine groups in the SAM for the formation of Au^{3+}@SAM/MCF-17.[12,20,21] The solid catalyst was washed three times in order to remove the residual Au ions that were not encapsulated in the SAM. The encapsulated Au ions were reduced to nanoparticles by exposure to 1 atm of H_2 at 40 °C for 24 h. XPS measurements verified the metallic properties of the gold clusters (Supporting Information, Figure S2). HR-TEM analysis indicated the formation of monodispersed Au clusters with diameter of 6 ± 1 nm with loading of 0.4 w/w % Au in proline/MCF-17. Increasing the amount of encapsulated Au by 5-fold to 2 w/w % led to bimodal distribution of the Au clusters, with small Au clusters (2 ± 0.5 nm) and large Au aggregates (20 ± 4 nm) (Supporting Information, Figure S5).

2.2. Reactivity. The catalytic reactivity and selectivity of Au clusters embedded in SAM (Au@SAM/MCF-17) was studied by using propargyl pivalate **6** and styrene as reactants in cyclopropanation reaction that produces *cis* and *trans* diastereomers of cyclopropane **7**.[15,22] Employing 0.4 w/w % Au encapsulated in (L)-proline/MCF-17 (proline **1** was attached to the surface through the OH terminal due to Boc protection of the amine) and 10 mol % $PhICl_2$ as an oxidizer, led to 87% conversion of **6** after 12 h, using toluene as a solvent (Table 1, entry 1). The selectivity toward the formation of cyclopropane **7** was 84%, while 16% of **6** was converted to the aldehyde (3-methyl-2-butenal) **8** byproduct. A *cis:trans* ratio of 10:1 and 14% ee of cyclopropane **7** were measured.

Table 1. Au@SAM/MCF-17 Catalyzed Intermolecular Cyclopropane Synthesis[a]

entry	chiral molecule in SAM	loading (w/w %)[b]	conversion (%)[c]	chemoselectivity (cis/trans-7: aldehyde 8) (%:%)	diastereoselectivity (cis-7:trans-7)	ee (%)
1	proline **1**[d]	0.4	87	84:16	10:1	14
2	hydroxyproline **2**	0.4	45	86:14	5:1	17
3	diproline **3**	0.4	85	89:11	9:1	51
4	proline **1**	2	70	80:20	6:1	4
5	proline **1** (N anchored)	0.4	8	65:35	3:1	0
6	unsupported diproline[e]	NA	15	75:25	5:1	0
7	phenylalanine **4**	0.4	85	82:18	6:1	5
8	quinine **5**	0.4	<1			

[a]The reactions were performed at room temperature, using toluene as a solvent. The reactants and oxidizer amounts were 0.15 and 0.015 mmol, which are two and one order of magnitude higher than that of the Au catalyst, respectively. [b]Loading was measured by ICP-MS. [c]Conversion, selectivity, and diastereoselectivity were measured by ^{1}H NMR after 12 h. [d]Proline was anchored to the surface through the OH group. [e]3 mol % of $AuCl_3$ was mixed with 10 mol % Pro-Pro-OMe·HTFA and 10 mol % Et_3N in toluene.

Inductively Coupled Plasma Mass Spectrometry (ICP-MS) measurements did not detect any leaching of Au ions to the solution phase following the reaction. Leaching of the highly reactive Au(III) ions was prevented by the repulsion forces between the hydrophilic catalyst and hydrophobic solvent.[23,24] Solution phase Au ions are expected to be highly active, when compared to the embedded Au clusters, and as a consequence, any enantioselectivity would be diminished by leaching of a small quantity of Au ions to the solution.[15] Therefore, the measured enantioselectivity values confirm the stability of the highly oxidized Au ions within the SAM.

An increase in the enantioselectivity to 17% ee was measured by substituting the SAM of proline **1** with that of hydroxyproline **2** (Table 1, entry 2). The increase in the enantioselectivity can be attributed to better packing of the SAM around the active Au clusters as a result of the formation of hydrogen-bonding network in the SAM by the hydroxy group of the hydroxyproline **2**. The presence of OH and carboxylic-ester signals in DRIFTS spectra indicated that the hydroxyproline was attached to the surface through the carboxylic terminal.

On the basis of this hypothesis, diproline **3** was synthesized and immobilized on MCF-17. The potential advantages in replacing the amino acid with a dipeptide are the addition of another chiral center and the construction of hydrogen-bonding network in the SAM. High reactivity and selectivity toward the formation of cyclopropane **7** was obtained using Au@diproline/MCF-17 catalyst, with cis:trans ratio of 9:1 and 51% ee (Table 1, entry 3). The immobilization of triproline did not lead to further enhancement in the products selectivity (Figure 1a, black curve). In a previous study, we showed that the diastereoselectivity values of the product cyclopropane are correlated to the packing density of the matrix that coats the Au cluster.[15] In a similar way, it was observed here that the formation of highly packed matrix around the Au clusters favors the cis diastereomer due to steric effect.[20]

Increasing the Au loading to 2 w/w % in Au@proline/MCF-17 deteriorated the catalytic reactivity and selectivity with cis:trans ratio and ee values of 6:1 and 4%, respectively (Table 1, entry 4). HR-TEM imaging indicated that Au aggregates with diameter of up to 20 nm were formed due to the increase in Au loading (Supporting Information, Figure S5). These aggregates were not fully embedded in the chiral matrix, resulting in a decrease in the selectivity while employing 2 w/w % Au@proline/MCF-17 as catalyst.
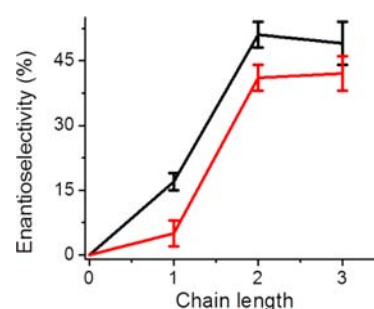

Figure 1. The intermolecular enantioselective formation of cyclopropane **7** as function of the number of proline (black) and phenylalanine (red) units in the chain molecule that construct the SAM. 3-fold enhancement in the enantioselectivity was obtained when the amino acid was replaced with a dipeptide in the SAM of the Au@SAM/MCF-17 catalyst. Error bars represent up to ±6% differences in reproducibility.

Low catalytic reactivity (8% yield) and selectivity (3:1 cis:trans ratio and no enantioselectivity) were obtained with 0.4 w/w % Au@proline/MCF-17 while immobilizing the (L)-proline **1** through its NH terminal (Table 1, entry 5). In this case, an unprotected (L)-proline **1** was employed for the formation of SAM and the attachment through the NH terminal was verified by DRIFTS spectra.

The importance of amine groups as an initial nucleation point for the formation of nanoparticles was previously demonstrated for dendrimer-encapsulated metal nanoclusters.[20] As observed here as well, the accessibility of the amine group is a key parameter for the preparation of Au ion–proline complexes prior to the clusters growth step. Alkylation of proline through the amine group hinders, by either electronic or steric effects, the complexation step. As a consequence, most of the Au ions were lost in the washing process of the catalyst (prior to clusters reduction), resulting in low reactivity and selectivity.

Low yield and no enantioselectivity were measured while employing diproline as an ancillary ligand with Au ions (Table 1, entry 6). The low reactivity of the homogeneous analogue to the active heterogeneous catalyst was correlated to strong interactions between Au ions and diproline molecules which prevent the catalytic formation of cyclopropane.[16]
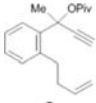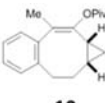
Mixing the racemic mixture of cyclopropane **7** with Au@diproline/MCF-17 catalyst for 10 h in toluene did not lead to asymmetric separation, excluding any role of the chiral SAM in preferred separation of one enantiomer over the other. No product was detected while employing diproline/MCF-17 (without the Au clusters) as catalyst. Au@diproline/MCF-17 was not active without the addition of an oxidizer. These experiments further support the hypothesis that Au(III) ions are the catalytically active species in this reaction.

Diastereoselectivity and enantioselectivity values of 6:1 and 5% were measured when 0.4 w/w % Au@phenylalanine/MCF-17 was employed as catalyst (Table 1, entry 7). Increasing the number of phenylalanine units in the immobilized peptide from 1 to 2 and 3 increased the enantiomeric excess of the cyclopropane from 7 to 42 and 44, respectively (Figure 1a, red curve).

Though quinine **5** is widely used as a chiral ligand for a variety of asymmetric heterogeneous catalytic reactions, in this case, almost no reactivity (<1%) was obtained while using Au@quinine/MCF-17 as catalyst (Table 1, entry 8).

The Au@SAM/MCF-17 catalyst was also tested for intramolecular cyclopropanation reaction.[25] Using 0.4 w/w % Au@proline/MCF-17 as catalyst, 74% conversion of **9** and 10% ee of cyclopropane product **10** were measured (Table 2, entry

Table 2. Au@SAM/MCF-17 Catalyzed Intramolecular Cyclopropane Synthesis

	chiral molecule in SAM	conversion (%)[a]	ee (%)
1	proline	74	10
2	diproline	39	39
3	phenylalanine	85	7
4	diphenylalanine	93	26

[a]Reactions performed at room temperature, using toluene as a solvent and 0.4 w/w % loading of Au. The reactant **9** and $PhICl_2$ amounts were 0.15 and 0.015 mmol, which are 2 and 1 order of magnitude higher than that of the Au catalyst, respectively. The yield and ee values were measured by ^{1}H NMR and chiral HPLC after 12 h.

1). Replacing the amino acid with a dipeptide increased the reactivity and enantioselectivity to 95% and 30%, respectively (Table 2, entry 2). Lower ee values were obtained while using phenylalanine instead of proline for chiral SAM, with 7% and 26% ee of cyclopropane **10** with SAM of phenylalanine and diphenylalanine, respectively (Table 2, entries 3 and 4). As in the intermolecular cyclopropanation reaction, preparing SAM with longer peptides did not lead to any further enhancement in the products selectivity.

It should be noted that the Au clusters diameter (6 ± 1 nm) is larger than the length of the peptide in the SAM (~1.5 nm). However, the encapsulation of Au clusters inside the three-dimensional pores of the mesoporous SiO_2 prevented leaching of Au ions to the solution phase, while enabling the diffusion of reactants to the catalyst. No enantioselectivity was measured when Pd@diproline/MCF-17 was used as a catalyst for hydrogenation reactions, since the active catalysts in these reactions are the metallic nanoclusters which are not entirely shielded by the chiral SAM. In contrast, in the cyclopropanation reactions the active catalysts are the highly oxidized metal ions

which are well encapsulated in the SAM due to electronic interaction with the nucleophilic groups in the SAM, enabling the diastereo- and enantioselective cyclopropanation reaction.

2.3. Spectroscopic Characterization. X-ray absorption spectroscopy (XAS) measurements were conducted at beamline 10.3.2 of the Advanced Light Source (ALS) at Lawrence Berkeley National Laboratory in order to characterize the active species in the Au@diproline/MCF-17 catalyst. The data were collected in fluorescence mode at the Au L_3 edge (11.918 keV). In situ NEXAFS (Near Edge X-ray Absorption Fine Structure) spectroscopy of the reduced catalyst (1 w/w % Au@diproline/MCF-17) dissolved in toluene (Figure 2, curve a) indicated the
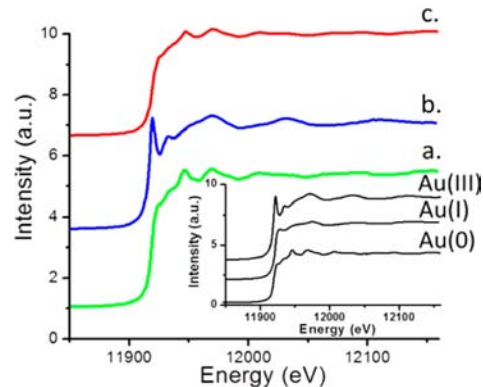

Figure 2. In situ NEXAFS spectra of reduced (a) and oxidized (b) Au@diproline/MCF-17 in toluene. The Au clusters were oxidized by the addition of 10 mol % $PhICl_2$ to the solution phase. Following the addition of oxidizer, the Au(0) clusters were oxidized to Au(III). After mixing the oxidized catalyst (b) with the reactants for 12 h, another NEXAFS spectrum was measured (c), which indicated the reduction of Au back to its metallic state. Reference NEXAFS spectra of Au(0) (Au foil), Au(III) ($AuCl_3$), and Au(I) ((Ph_3P)AuCl) are shown in the inset.

presence of metallic Au(0) clusters. The addition of 10 mol % $PhICl_2$ to the solution oxidized the gold clusters to Au(III) (Figure 2, curve b). The catalyst was then mixed with the reactants for 12 h, after which 90% yield of cyclopropane with *cis*:*trans* ratio of 10:1 was measured. NEXAFS data (Figure 2, curve c) indicated that following the catalytic reaction, the Au ions were reduced to their metallic state, resulting in the deactivation of the catalyst.

In situ NEXAFS measurements under reaction conditions indicated that the formation of highly oxidized Au(III) ions is directly correlated to the formation of products. It was also obtained that the catalytic rate decreased along with the reduction of Au(III) ions (Supporting Information, Figure S6). These results are consistent with our previous observations that the active catalysts for this reaction are the highly oxidized Au(III) ions.

Following the deactivation, the catalytic activity was regained by reoxidizing the metallic clusters with the addition of 10 mol % $PhICl_2$ to the solution phase. Only minor differences in clusters properties and their catalytic reactivity were obtained when comparing the original and the recycled catalysts.[15,23,24]

The properties of the SAM/MCF-17 were analyzed by TGA-MS (Thermal Gravimetric Analysis Mass Spectrometry) measurements, performed under thermal treatment with oxidative conditions and a temperature ramp of 5 deg/min. The combustion temperature, defined by the rate of mass loss, reflects the SAM properties.[26] The first derivative of mass loss

of Br/MCF-17 indicated that the SAM is combusted at 250 °C (Figure 3, curve a). The esterification of proline on Br/MCF-17
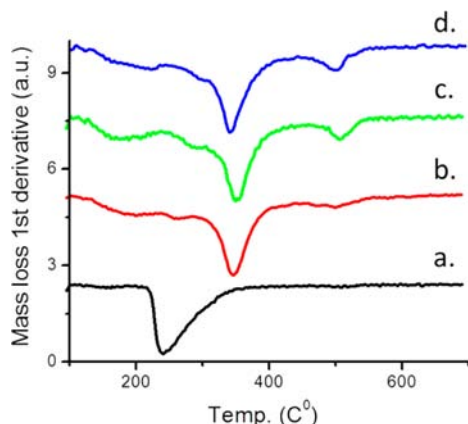

Figure 3. Thermal gravimetric analysis (TGA) first derivative curve for Br/MCF-17 (a), proline/MCF-17 (b), diproline/MCF-17 (c), and triproline/MCF-17 (d). The minima in the TGA curve are correlated to combustion of the SAM. The immobilization of proline on the Br/MCF-17 stabilized the SAM. Comparison of the diproline/MCF-17 and proline/MCF-17 TGA spectra indicates that the SAM is further stabilized due to addition of another proline to the peptide chain.

stabilized the SAM and the decomposition temperature of proline/MCF-17 increased by 100 to 355 °C (Figure 3, curve b). The SAM was further stabilized by the addition of another proline unit to the peptide chain. TGA spectra of diproline/MCF-17 and triproline/MCF-17 (curves c and d in Figure 3, respectively) indicated the formation of an additional high-temperature combustion peak at 510 °C. By increasing the number of proline units above one the SAM was further stabilized, presumably due to interactions between the peptides. Encapsulation of Au clusters in the SAM (Au@diproline/MCF-17) did not lead to any modifications in the TGA spectra.

TGA-MS analysis of 30 m/z (correlated to the formation of NO molecules) indicated that the high-temperature mass loss peak (510 °C) detected in the TGA spectra is due to combustion of the amino acid (Supporting Information, Figure S7). The interactions within the molecules in the SAM, which are in high proximity to the catalytically active Au ions, lead to better packing of chiral molecules that favor specific orientation of the reactants. These interactions result in the enhancement in the diastereoselectivity and enantioselectivity values of products **7** and **10**.

The nature of the interactions between the peptides in the SAM was studied by DRIFT spectroscopy. As the number of proline units in the peptide that construct the SAM was increased, a broad peak between 2800 and 3700 cm^{-1} was detected, which is correlated to inter- and intramolecular hydrogen bonding (Figure 4, curves b−d).[27,28] The increase in the IR abosprtion peak in this region indicates that the stabilization of the diproline/MCF-17 and triproline/MCF-17, detected in the TGA-MS spectra, can be correlated to the formation of hydrogen bonding network in the SAM.

Combining the catalytic and spectroscopic data, it can be concluded that the 3-fold enhancement in the enantioselectivity obtained by substituting proline with diproline SAM is due to better packing and stabilization of the SAM around the active catalyst. The highly packed diproline SAM favors specific symmetry of the reactant as it approaches the catalytically active
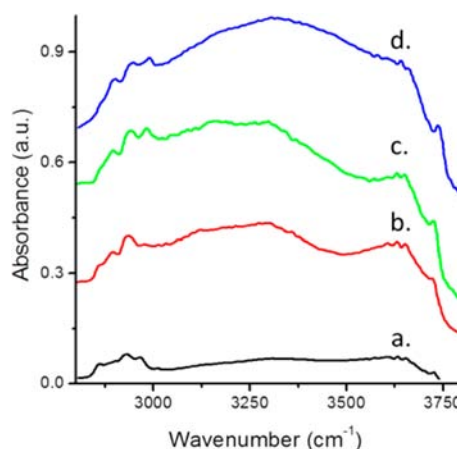

Figure 4. DRIFT spectroscopy of Br/MCF-17 (a), prolin/MCF-17 (b), diproline/MCF-17 (c), and triproline/MCF-17 (d). The samples were annealed to 70 °C under vacuum for 24 h, in order to ensure the removal of adsorbed water molecules. Increasing the number of proline links in the chain is followed by an increase in the DRIFTS peak between 2800 and 3700 cm^{-1}, which is correlated to intermolecular and intramolecular hydrogen bonding in the SAM.

Au ions through the SAM, which results in the increase in product selectivity.

3. CONCLUSIONS

Diastereoselective and enantioselective heterogeneous Au catalysts for cyclopropanation reactions have been developed by immobilization of chiral SAM on the surface of mesoporous SiO$_2$ support. Complexation of Au ions within the SAM enabled the formation of Au clusters that are encapsulated in the chiral SAM. The Au@SAM/MCF-17 catalyst was activated through metal oxidation by PhICl$_2$. Under these conditions, Au@diproline/MCF-17 catalyzed intermolecular and intra-molecular cyclopropanation reactions with up to 51% and 30% enantiomeric excess, respectively. In the case of the intermolecular cyclopropanation reaction, the enantioselectivity was coupled with high diastereoselectivity. NEXAFS analysis indicated that highly oxidized Au(III) species are the active species in this reaction. Spectroscopic analysis of the SAM/MCF-17 revealed that as the number of amino acids in the molecules that construct the SAM is increased above one, the SAM is stabilized due to the formation of hydrogen-bonding network. The intermolecular and intramolecular hydrogen bonding of the SAM favors specific alignment of the reactant as it approaches through the SAM to the catalytically active Au ions.

These results demonstrate the advantages of mesoscale catalysts that assemble together two different building blocks for the formation of an architecturally designed catalyst. In this case, the combination of metallic nanoclusters and chiral SAM matrix enabled the preparation of reactive and enantioselective heterogeneous catalysts. Unlike other asymmetric heteroge-neous catalysts, in which ligand−reactants interactions are needed for asymmetric reactions, by using the chiral SAM, the enantioselectivity is enhanced due to the chirality of the matrix. It should be noted that in this study only a few chiral molecules were tested for the formation of SAM as an initial proof of concept for employing this system for asymmetric reactions. Preparation of SAM with other homopeptides or heteropep-tides may lead to better catalytic reactivity and selectivity. The

use of a robotic system for the preparation of a library of peptides is planned in order to gain a better scope of the SAM-based mesoscale catalyst.

ASSOCIATED CONTENT

Supporting Information

Details of the experimental procedure and spectroscopic and microscopic data. This material is available free of charge via the Internet at http://pubs.acs.org.

AUTHOR INFORMATION

Corresponding Author
fdtoste@berkeley.edu, somorjai@berkeley.edu

Notes
The authors declare no competing financial interest.

ACKNOWLEDGMENTS

REFERENCES

(1) Ringe, D.; Petsko, G. A. *Science* **2008**, *320*, 1428.
(2) Reek, J. N. H.; Meeuwissen, J. *Nat. Chem.* **2010**, *2*, 615.
(3) (a) Mallat, T.; Orglmeister, E.; Baiker, A. *Chem. Rev.* **2007**, *107*, 4863. (b) Heitbaum, M.; Glorius, F.; Escher, I. *Angew. Chem. Int. Ed.* **2006**, *45*, 4732.
(4) Kyriakou, G.; Beaumont, S. K.; Lambert, R. M. *Langmuir* **2011**, *27*, 9687.
(5) Han, D.; Li, X.; Zhang, H.; Liu, Z.; Li, J.; Li, C. *J. Catal.* **2006**, *243*, 318.
(6) Smejkal, T.; Breit, B. *Angew. Chem., Int. Ed.* **2008**, *47*, 311.
(7) Gustafson, J. L.; Lim, D.; Miller, S. J. *Science* **2010**, *328*, 1251.
(8) Uraguchi, D.; Ueki, Y.; Ooi, T. *Science* **2009**, *329*, 120.
(9) Breit, B.; Seiche, W. *Angew. Chem., Int. Ed.* **2005**, *44*, 1640.
(10) Milo, A.; Neumann, R. *Chem. Commun.* **2011**, *47*, 2535.
(11) Cortial, G.; Goettmann, F.; Mercier, F.; Le-Floch, P.; Sanchez, C. *Catal. Commun.* **2007**, *8*, 215.
(12) Datta, K. K. R.; Reddy, B. V. S.; Ariga, K.; Vinu, A. *Angew. Chem., Int. Ed.* **2010**, *49*, 5961.
(13) Wu, B.; Huang, H.; Yang, J.; Zheng, N.; Fu, G. *Angew. Chem., Int. Ed.* **2012**, *51*, 3440.
(14) Marshall, S. T.; O'Brien, M.; Oetter, B.; Corpuz, A.; Richards, R. M.; Schwartz, D. K.; Medlin, J. W. *Nat. Mater.* **2010**, *9*, 853.
(15) Gross, E.; Liu, J. H.; Toste, F. D.; Somorjai, G. A. *Nat. Chem.* **2012**, *4*, 947.
(16) Gross, E.; Krier, J. M.; Heinke, L.; Somorjai, G. A. *Top. Catal.* **2012**, *55*, 13.
(17) Li, Y. M.; Liu, J. H. C.; Witham, C. A.; Huang, W. Y.; Marcus, M.; A. Fakra, S. C.; Alayoglu, P.; Zhu, Z. W.; Thompson, C. M.; Arjun, A.; Lee, K.; Gross, E.; Toste, F. D.; Somorjai, G. A. *J. Am. Chem. Soc.* **2011**, *133*, 13527.
(18) Tsung, C. K.; Khun, J. N.; Huang, W. Y.; Aliaga, C.; Hung, L.; Somorjai, G. A.; Yang, P. D. *J. Am. Chem. Soc.* **2009**, *131*, 5816.
(19) Climent, M. J.; Corma, A.; Iborra, S.; Navarro, M. C.; Primo, J. *J. Catal.* **1996**, *161*, 783.
(20) Borodko, Y.; Thompson, C. M.; Huang, W. Y.; Yildiz, H. B.; Frei, H.; Somorjai, G. A. *J. Phys. Chem. C* **2011**, *115*, 4757.
(21) Borodko, Y.; Habas, S. E.; Koebel, M.; Yang, P. D.; Frei, H.; Somorjai, G. A. *J. Phys. Chem. B* **2006**, *110*, 23052.
(22) Johansson, M. J.; Gorin, D. J.; Staben, S. T.; Toste, F. D. *J. Am. Chem. Soc.* **2005**, *127*, 18002.
(23) Huang, W. Y.; Liu, J. H. C.; Alayoglu, P.; Li, Y.; Witham, C. A.; Tsung, C. K.; Toste, F. D.; Somorjai, G. A. *J. Am. Chem. Soc.* **2010**, *132*, 16771.
(24) Witham, C. A.; Huang, W. Y.; Tsung, C. K.; Kuhn, J. N.; Somorjai, G. A.; Toste, F. D. *Nat. Chem.* **2010**, *2*, 36.
(25) Watson, I. D. G.; Ritter, S.; Toste, F. D. *J. Am. Chem. Soc.* **2009**, *131*, 2056.
(26) Gazit, O. M.; Katz, A. *Langmuir* **2012**, *28*, 431.
(27) Fabris, L.; Antonello, S.; Armelao, L.; Donkers, R. L.; Polo, F.; Toniolo, C.; Maran, F. *J. Am. Chem. Soc.* **2006**, *128*, 326.
(28) Bertilsson, L.; Liedberg, B. *Langmuir* **1993**, *9*, 141.